AGU PUBLICATIONS

JGR

Journal of Geophysical Research: Space Physics

RESEARCH ARTICLE
10.1002/2015JA021373

Effects of Saturn's magnetospheric dynamics on Titan's ionosphere

N. J. T. Edberg[1,2], D. J. Andrews[1], C. Bertucci[3], D. A. Gurnett[2], M. K. G. Holmberg[1], C. M Jackman[4], W. S. Kurth[2], J. D. Menietti[2], H. J. Opgenoorth[1], O. Shebanits[1], E. Vigren[1], and J.-E. Wahlund[1]

[1]Swedish Institute of Space Physics, Uppsala, Sweden, [2]Department of Physics and Astronomy, University of Iowa, Iowa City, Iowa, USA, [3]IAFE, Buenos Aires, Argentina, [4]University of Southampton, Southampton, UK

Abstract We use the Cassini Radio and Plasma Wave Science/Langmuir probe measurements of the electron density from the first 110 flybys of Titan to study how Saturn's magnetosphere influences Titan's ionosphere. The data is first corrected for biased sampling due to varying solar zenith angle and solar energy flux (solar cycle effects). We then present results showing that the electron density in Titan's ionosphere, in the altitude range 1600–2400 km, is increased by about a factor of 2.5 when Titan is located on the nightside of Saturn (Saturn local time (SLT) 21–03 h) compared to when on the dayside (SLT 09-15 h). For lower altitudes (1100–1600 km) the main dividing factor for the ionospheric density is the ambient magnetospheric conditions. When Titan is located in the magnetospheric current sheet, the electron density in Titan's ionosphere is about a factor of 1.4 higher compared to when Titan is located in the magnetospheric lobes. The factor of 1.4 increase in between sheet and lobe flybys is interpreted as an effect of increased particle impact ionization from ~200 eV sheet electrons. The factor of 2.5 increase in electron density between flybys on Saturn's nightside and dayside is suggested to be an effect of the pressure balance between thermal plus magnetic pressure in Titan's ionosphere against the dynamic pressure and energetic particle pressure in Saturn's magnetosphere.

Key Points:
- Saturn's magnetosphere affects Titan's ionosphere, revealed after solar cycle and SZA effects removed
- Influence from Saturn magnetosphere different on topside and deep ionosphere
- Topside ionosphere influenced by pressure balance, deep ionosphere by sheet, or lobe conditions

Correspondence to:
N. J. T. Edberg,
ne@irfu.se

Citation:
Edberg, N. J. T., et al. (2015), Effects of Saturn's magnetospheric dynamics on Titan's ionosphere, *J. Geophys. Res. Space Physics*, *120*, 8884–8898, doi:10.1002/2015JA021373.

Received 24 APR 2015
Accepted 18 SEP 2015
Accepted article online 22 SEP 2015
Published online 12 OCT 2015

1. Introduction

Saturn's largest moon Titan has a dense and extended atmosphere, mainly populated by N_2 and CH_4 but with a wealth of less abundant species present, including heavy organic molecules. Titan is the only moon in the solar system with such a dense atmosphere. It is particularly interesting to study since the atmosphere reminds that of the early Earth, before life evolved. Plasma processes in the upper part of Titan's ionized atmosphere are crucial to study if we want to understand the evolution of Titan's atmosphere and ionosphere.

The neutral particles in Titan's atmosphere are ionized mainly by the extreme ultraviolet (EUV) radiation from the Sun and to a lesser extent from impacting energetic particles and charge exchange processes, and a complex exosphere and ionosphere are formed. The ionosphere is dominated by $HCNH^+$ and $C_2H_5^+$ ions [*Cravens et al.*, 2006; *Vuitton et al.*, 2007], while many other ion species exists, including heavy positive and negative ions [*Coates et al.*, 2007; *Coates*, 2009; *Waite et al.*, 2007; *Crary et al.*, 2009; *Wahlund et al.*, 2009; *Ågren et al.*, 2012; *Shebanits et al.*, 2013; *Wellbrock et al.*, 2013]. The complex chemistry in the ionosphere eventually leads to the formation of aerosols and heavy organic molecules [*Lavvas et al.*, 2013] out of which some are deposited on the surface of the moon. To fully understand this process, it is important to understand all sources of ionization at Titan as well as what drives the dynamics in Titan's upper atmosphere and ionosphere.

Titan's ionosphere was first observed by measurements from the Voyager flyby [*Bird et al.*, 1997], and since the arrival of Cassini in 2004 and its many flybys of the moon, the knowledge has increased significantly. *Wahlund et al.* [2005] presented the first measurements of the cold plasma properties in the ionosphere from the first two flybys, TA and TB. *Backes et al.* [2005] presented the first magnetic field measurements from the induced magnetosphere of Titan, which is formed as the corotating magnetosphere of Saturn interacts with the ionosphere of Titan.

Titan orbits Saturn at a distance of about 21 R_S (1 R_S = 60,268 km) with an orbital period of about 16 days. The corotating flow in Saturn's magnetosphere is subsonic, and so no bow shock is formed upstream of

Titan, while a weak pileup of draped magnetic field and an induced magnetosphere is formed. Several modeling efforts have been undertaken to understand the structure and formation of Titan's ionosphere. *Cravens et al.* [2006] and *Ågren et al.* [2007] both studied magnetospheric impact ionization and found that it was a likely contributor to especially the Titan nightside ionosphere. *Cravens et al.* [2008] showed that precipitating ions could contribute significantly to the ionization at and below the peak altitude ($\sim$1100 $\pm$ 100 km). Solar EUV is, however, the dominating source for ionization on the dayside [*Ågren et al.*, 2009; *Edberg et al.*, 2013a; *Vigren et al.*, 2013], while electron impact ionization has been shown to be more important on the nightside [*Ågren et al.*, 2007; *Vigren et al.*, 2015].

The variability of the structure of Titan's ionosphere and induced magnetosphere is large, partly due to the large variations in the ambient plasma and field conditions in Saturn's magnetosphere [*Rymer et al.*, 2009; *Smith and Rymer*, 2014; *Simon et al.*, 2010, 2013]. These authors found that Titan can be located either in the magnetodisc current sheet, which is filled with $\sim$200 eV electrons [*Arridge et al.*, 2009], or in the less dense but hotter magnetospheric lobe or in a mixture of different ambient conditions. From those studies it can be concluded that dynamics in the ambient plasma conditions are present and substantial on both the dayside and on the nightside of Saturn. The ambient plasma conditions can change on timescales shorter than the length of a flyby through the ionosphere ($\sim$30 min). *Luhmann et al.* [2012] tried to disentangle magnetospheric effects on Titan from the first 6 years of measurements (60 flybys) using a multi-instrument approach and mainly studied data below an altitude of 1400 km. They concluded that the variability was large and that many factors contributed to the variability without being able to see any systematic trends. *Westlake et al.* [2011] looked at thermospheric (altitude range 1000–1500 km) densities for various ambient conditions. They found that when Titan was located in the plasma sheet, the thermospheric neutral density was significantly higher than when Titan was located in the magnetospheric lobes.

Titan is normally located within Saturn's magnetosphere and mostly encounters magnetospheric plasma and fields as it orbits the planet. However, on the dayside of Saturn, the solar wind dynamic pressure will occasionally push the Saturn magnetopause, which has a typical standoff distance of 22–27 R_S [*Achilleos et al.*, 2008], closer to the planet. If Titan is located close enough to the subsolar point of Saturn at that time, the magnetopause can move to inside of the orbit of Titan. Titan will then experience the plasma in the magnetosheath of Saturn, or even in the solar wind, rather than the magnetosphere. However, such events are rare. During the T32 flyby *Bertucci et al.* [2008] reported on the existence of long lasting draped magnetic field lines ("fossil fields") which stayed for several hours as Titan traversed the Saturn magnetopause. *Garnier et al.* [2009] also studied the T32 flyby in terms of plasma observations and pressure balance in the induced magnetosphere but found no significant alterations to its structure. From the T42 flyby *Wei et al.* [2011] reported on unusually high magnetic field strength and pressure in Titan's ionosphere and linked that to a high solar wind dynamic pressure event. *Edberg et al.* [2013b] studied the T85 flyby when Titan moved into the magnetosheath during a solar wind pressure pulse impact. They observed that the ionospheric electron densities were the highest ever observed at Titan during that pass, possibly due to increased particle impact ionization around the ionospheric peak altitude. There is a great variability in the Titan interaction with the ambient plasma which has enabled many case studies of individual flybys. Moreover, *Bertucci et al.* [2015] presented a unique case when Titan was located in the solar wind while Cassini performed a flyby through the induced magnetosphere of the moon. It was found that the Titan-solar wind interaction very much resembles that of Mars' and Venus'. Motion of the dayside plasma boundaries and regions is one reason for the observed variability in the ambient conditions, which in turn can modify the structure of Titan's ionosphere.

On the nightside of Saturn, there are other features in Saturn's dynamic magnetosphere that may influence Titan's plasma environment. The flapping (a temporal effect) and hinging (a seasonal effect) of the current sheet [e.g., *Arridge et al.*, 2011; *Simon et al.*, 2010], possibly driven by changing conditions in the upstream solar wind, will set Titan either in the lobe (north/south), plasma sheet, or in the middle of the current sheet itself. This ought to have an effect on the structure of the ionosphere and induced magnetosphere. The plasma flow patterns in Saturn's tail are predominantly in the corotation direction but have been observed to be somewhat asymmetric across midnight. In the postmidnight sector, the plasma flow was reported to deviate from the ideal corotational direction and the flow tended to be more tailward outside of about 30 R_S [*McAndrews et al.*, 2009, 2014]. Subsequently, *Thomsen et al.* [2013, 2014] used the same instrument but a different technique to obtain the plasma parameters. They found that most flows were in the corotational direction. In the premidnight sector there was some evidence of inward flow but a noteworthy lack of tailward-flowing plasma

(outflow), while in the postmidnight sector the situation was reversed, with some evidence of outward flow and little or no inward flow.

Furthermore, Saturn magnetospheric tail dynamics in terms of reconnection events, plasmoids, and traveling compression regions have been observed in the tail region of Saturn, and the occurrence rate has been shown to be asymmetric across midnight [*Jackman et al.*, 2011, 2014]. Following the model by *Cowley et al.* [2004], reconnection on closed field lines (associated with the Vasyliunas cycle) should occur predominantly in the dusk sector, while reconnection on open field lines (associated with the Dungey cycle) should occur on the dawn side. As *Thomsen et al.* [2013] found no evidence for outward flow in the dusk sector they suggested that the plasmoids formed from reconnection on the dusk side were trapped in outer closed field lines and released only when having reached the dawn flank and that once such plasma has passed midnight, reconnection of open field lines could begin and plasma could ultimately be released downtail.

Energetic neutral atoms (ENA) emissions are also a prominent feature in Saturn's magnetosphere [e.g., *Mitchell et al.*, 2005]. The ENA emission usually peaks inside the orbit of Titan, closer to 15 R_S where the energized particles from the tail interact with the neutral torus and are also asymmetric across midnight but with the peak intensities normally in the premidnight sector, for both energetic hydrogen and oxygen [*Carbary et al.*, 2008].

In this paper we will present results showing that the electron density in the ionosphere of Titan is dependent on the Saturn local time (SLT), as well as on the ambient magnetospheric conditions. The results are produced after we have corrected for biased sampling at different solar zenith angles (SZAs) and phases of the solar cycle.

2. Instruments and Orbital Geometry

The Cassini spacecraft carries the Radio and Plasma Wave Science/Langmuir probe (RPWS/LP) instrument [*Gurnett et al.*, 2004; *Wahlund et al.*, 2005]. The LP consists of a spherical shell with a diameter of 5 cm, which is fastened on a short stub. The stub and spherical shell are mounted on a boom extending 2 m away from the main spacecraft bus. During Titan flybys, the LP is normally run in "sweep mode" where the bias potential fed to the probe is swept from −4 to +4 V. Depending on the sign of the potential, the probe collects either ions or electrons and the resulting current is measured. One sweep is completed every 24 s. From the voltage-current characteristics physical parameters of the ambient plasma can be derived, such as electron density N_e and electron temperature T_e but also ion density, mean ion mass, and bulk flow speed as well as spacecraft potential. In this paper we will solely use the electron density obtained from the sweeps. The error of the electron density estimates is typically within 10%, when the density is above 100 cm^{-3}. This error comes from tests of instrument performance. A density of 100 cm^{-3} is typically reached at an altitude of about 1500–2000 km above the surface of Titan. For lower densities the error would be higher and densities below about 5 cm^{-3} are not reliably detectable by the LP when in sweep mode. The theory behind going from current-voltage curves to physical plasma parameters is rather complicated and will not be described in any detail here. It follows the work of *Mott-Smith and Langmuir* [1926], *Medicus* [1962], *Whipple* [1965], and *Fahleson et al.* [1974] and is more thoroughly described, e.g., by *Edberg et al.* [2011], *Morooka et al.* [2011], and *Shebanits et al.* [2013]. Recent work has also shown that the LP under certain conditions is capable of detecting negative ions [*Ågren et al.*, 2012; *Shebanits et al.*, 2013], as well as energetic electrons [*Garnier et al.*, 2013].

In this study we will also use solar energy flux F_e measurements from the solar EUV experiment (SEE) on the Thermosphere Ionosphere Mesosphere Energetics and Dynamics (TIMED) spacecraft, which is in orbit around the Earth [*Woods et al.*, 2005]. The TIMED/SEE instrument measures the spectral irradiance of the Sun, which is integrated to solar energy flux for wavelengths up to 90 nm (90 nm being the ionization threshold of N_2). We use daily averages of those measurements extrapolated to the orbit of Saturn. The extrapolation takes into account the solar rotation and radial distance, and a tool package for this is available on the TIMED-SEE webpage http://lasp.colorado.edu/lisird/tools.html.

We will also use the in situ magnetic field measurements from the magnetometer (MAG) on Cassini, downsampled to 1 min resolution [*Dougherty et al.*, 2004].

The coordinate systems used in this paper are the Titan interaction (TIIS) coordinate system and the ecliptic coordinate system. In the TIIS system the *x* axis is parallel to the corotational flow direction, the *y* axis is directed toward Saturn, and the *z* axis completes the right-handed system. In the Titan centered ecliptic coordinate

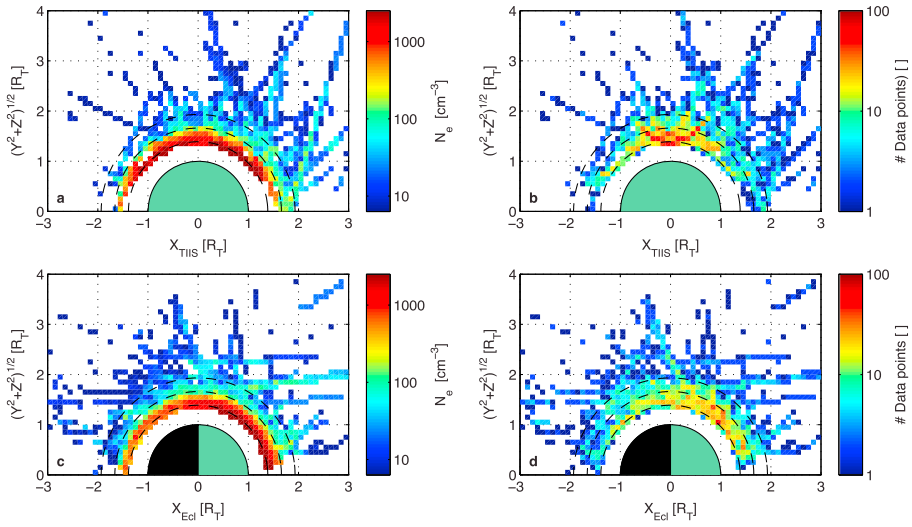

Figure 1. RPWS/LP measured electron density averaged in 0.1 × 0.1 R_T bins around Titan in (a) cylindrical TIIS coordinates together with (b) number of data points in each bin. (c and d) The same as shown in Figures 1a and 1b but in cylindrical ecliptic coordinates. The data is gathered from flyby TA to T109. Altitudes of 1000 km, 1700 km, and 2400 km are indicated by black dashed circles.

system, the *x* axis points toward the Sun, the *y* axis is formed by the cross product of the *x* axis and the normal to Titan's orbital plane, and the *z* axis completes the right-handed system.

3. Observations of Titan's Cold Electron Plasma

Figure 1 shows the electron density measured by RPWS/LP color coded on a map in cylindrical coordinates, in both the TIIS (Figure 1a) and in the ecliptic coordinate system (Figure 1c) to illustrate the data coverage and the general structure of the cold ionospheric plasma around Titan. The measurements from all Titan flybys that have occurred until February 2015 are included (TA–T109). The electron density is averaged in bins over 0.1 × 0.1 R_T (1 R_T = 2575 km), and the number of data points in each bin is displayed in Figures 1b and 1d, respectively. Only densities above 5 cm^{-3} are included. One can see from Figure 1a that the cold ionospheric plasma above the ionospheric main layer has generally been transported in the downstream direction and reach densities above 10 cm^{-3} well beyond 2 R_T during some flybys. On the ram side, high density at such high altitude is much rarer, if existing at all. The corotating plasma flow from Saturn's magnetosphere is evidently driving lots of the dynamics in the upper parts of Titan's exosphere/ionosphere. In Figure 1c the ionospheric density on the dayside in the ionosphere proper, at a distance below 2 R_T from the centre of the moon, is clearly much higher than the nightside values. This illustrates how the solar radiation is the main ionization source on the dayside of Titan.

To illustrate the dependence on solar radiation, SZA, and ram angle in more detail, we show in Figure 2 the electron density as a function of altitude and solar energy flux F_e (Figure 2a), SZA (Figure 2c), ram angle (Figure 2e), and the corresponding data density (Figures 2b, 2d, and 2f). In Figure 2a the electron density is averaged in bins of 1.5 μW m^{-2} × 75 km. The data density is uneven with more data points at lower solar energy flux. This is because most of the Titan flybys have occurred during the previous solar minimum (solar cycle 23/24) when the solar fluxes were low. Nevertheless, up to an altitude of at least ~1700 km, the density seems to increase with increasing solar energy flux. Figure 2c shows the same density measurements but now as a function of SZA and altitude and averaged in bins of 5° × 50 km. The number of data points for these bins (Figure 2d) shows that there are more measurements toward lower SZAs, since more flybys have traversed the ionosphere on the dayside than on the nightside of Titan. The trend is still clear—the electron density is higher at lower SZAs and at lower altitudes. A similar plot has also been shown in [*Shebanits et al.*, 2013]. In fact, the dropoff in density with increasing SZA seems valid up to an altitude of about 2000 km or thereabout. In Figure 2e the density is shown as a function of altitude and ram angle and averaged in bins of 5° × 50 km. The ram angle is defined to be 0° in the direction antiparallel to the corotating flow and 180° in the direction parallel to the flow. Ram angles around 90° are significantly better sampled than elsewhere. At low altitudes

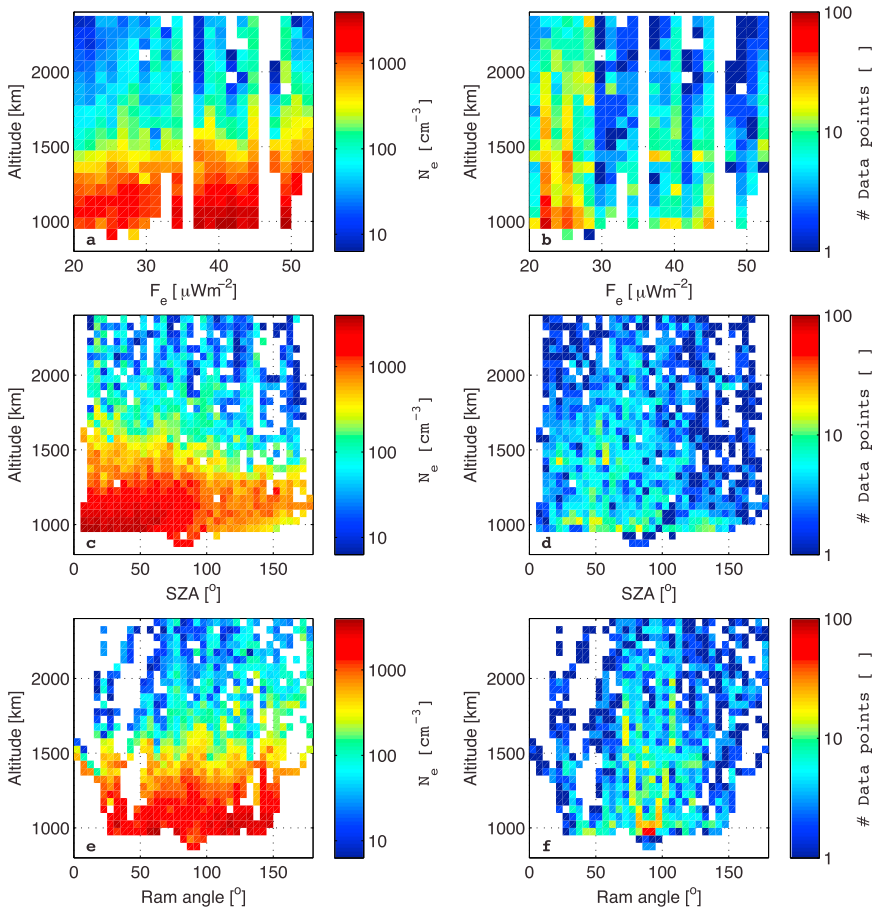

Figure 2. Electron density averaged in (a) 75 km × 1.5 μW m^{-2} altitude and solar energy flux bins, (c) in 50 km × 5° altitude and SZA angle bins, (e) in 50 km × 5° altitude and ram angle bins. (b, d, and f) Number of data points in each bin.

there does not appear to be any clear dependence on density with ram angles except near 1000 km and ram angle of 100–150°, where the density appears higher. However, these data points are also located at low SZAs where the photoionization is high and causes this higher density. At higher altitudes, above 1500 km, there is possibly a trend of increasing densities with increasing ram angle.

While there is an apparent, and already established, dependence of the ionospheric electron density on both solar radiation and SZA, there are other factors that could be important for controlling the structure of Titan's ionosphere. One such factor could be the dynamics in Saturn's magnetosphere. However, before we can test this we need to remove the dependence on solar energy flux and SZA. The Titan flybys that have occurred in the Saturn prenoon and postnoon sectors include, for instance, most of the flybys that have occurred since the beginning of the current solar maximum (of solar cycle 24) and have higher densities due to that [*Edberg et al.*, 2013a].

In the following sections we will describe how we remove the dependency on SZA and solar cycle and arrive at a data set which is independent of those two parameters and where the data has been shifted to represent values at the subsolar point and at solar minimum.

3.1. Removing the F_e, EUV and Ram Angle Dependence

First, since the peak altitude varies from flyby to flyby, we have shifted each individual altitude profile so that the peak altitude, i.e., where the electron density reaches maximum for each flyby, is always located at a common value, chosen to be the mean altitude of all the peaks at 1100 km. The altitude profiles have been shifted by adding or subtracting the altitude difference from 1100 km. After this we remove the dependence on SZA and solar energy flux, as described below.

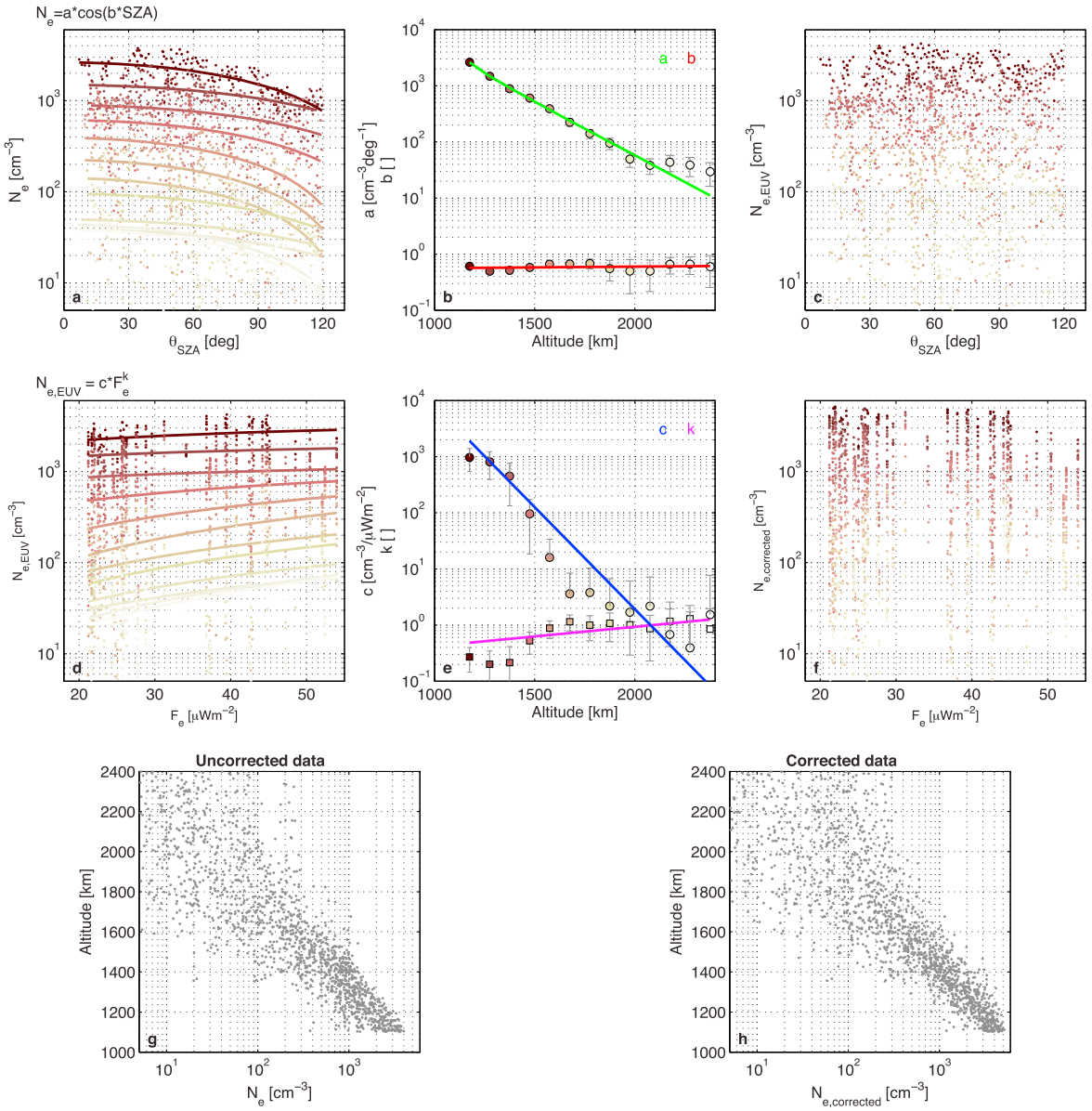

Figure 3. (a) Electron density as a function of SZA and color coded by altitude interval. Data from all SLT sectors are included. The colored lines show least squares fits to the data in 100 km altitude intervals, ranging from 1100 to 2400 km of the form as shown on the top of Figure 3a. (b) The parameters of the fits from Figure 3a as a function of altitude. The fits in Figure 3b are used to detrend the data from the SZA variation, and the result is shown in Figure 3c. (d–f) Same as for Figures 3a–3c but for solar energy flux rather than SZA. (g) The electron density altitude profiles with uncorrected data and (h) the electron density altitude profiles with corrected data.

According to Chapman theory, the density at the ionospheric peak, where photochemistry dominates, should decrease with SZA according to $N_e = a \cdot \cos^{1/2}(b \cdot \mathrm{SZA})$, where a is a free parameter and $b = 1$. However, at higher altitudes this relation might not strictly be a cosine dependence, and also, due to the extended exosphere of Titan, the SZA dependence is seen to extend to beyond a SZA = 90°. To investigate the SZA dependence at different altitudes, we plot the electron density N_e as a function of SZA in altitude intervals of 75 km in Figure 3a. We then fit curves of the form

$$n = a \cdot \cos(b \cdot \mathrm{SZA}) \tag{1}$$

to the data in each altitude range. The density follows the cosine dependence (rather than a $\cos^{1/2}$ dependence) at the lowest altitudes (darker lines) close to the peak altitude but also at higher altitudes. The parameters $a(r)$ and $b(r)$ of each of those fits are shown, as a function of altitude, in Figure 3b. The error bars

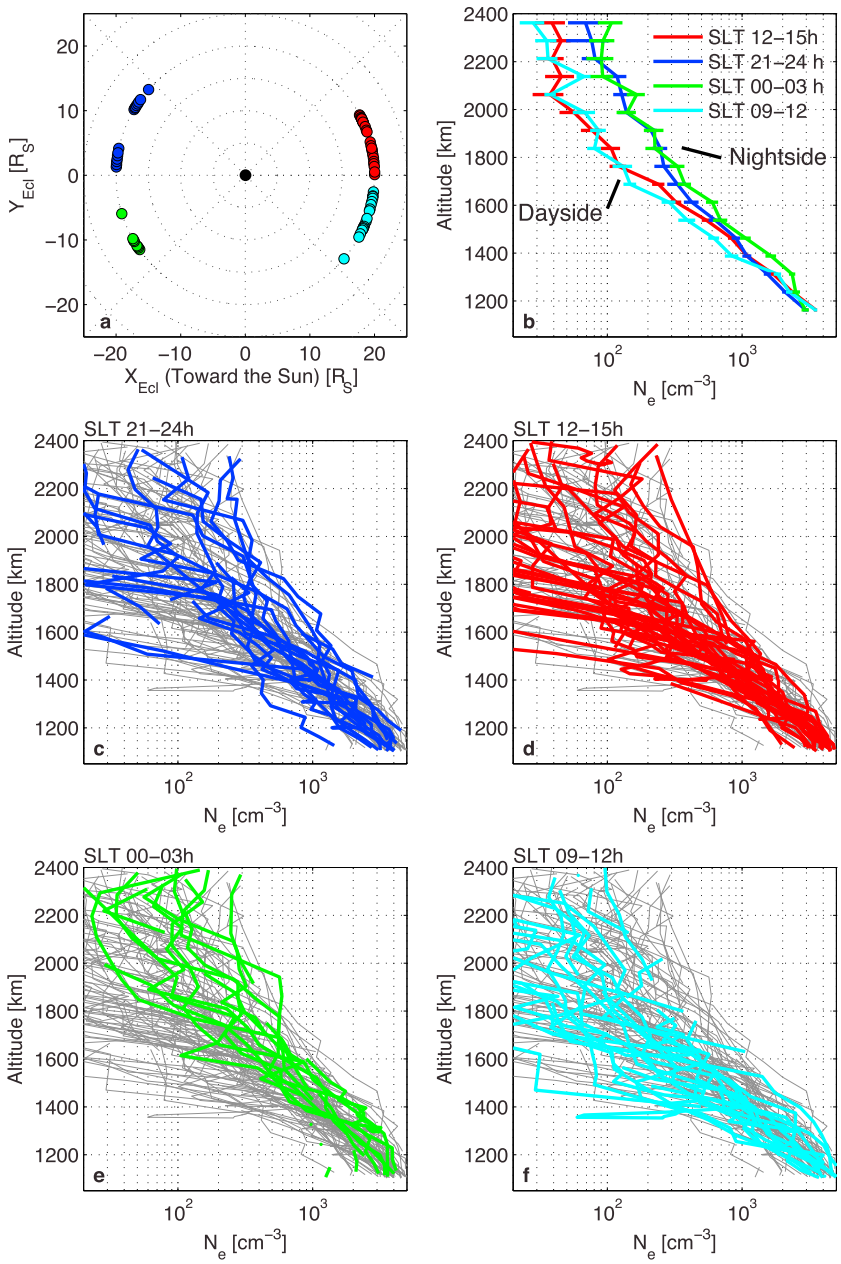

Figure 4. (a) Location of the Cassini Titan flybys shown projected on the *x-y* plane in the Saturn-centered ecliptic coordinate system. Noon is to the right, midnight to the left, dusk is up, and dawn is down in the figure. The colors correspond to in which SLT sector they occur. (b) Altitude profiles of the mean electron density (in altitude intervals of 75 km) from all the data retrieved in the respective SLT sectors. The data is corrected for solar cycle and SZA variations. (c–f) Each individual electron density altitude profile obtained by RPWS/LP from the respective SLT sector. The grey lines show all obtained altitude profiles from the Cassini mission for easier comparison between panels. Note that the electron density altitude profiles in the night sector (green and blue lines) stands out in terms of highest densities.

show the goodness of the fits. There is a clear exponential dependence on how the parameter $a(r)$ varies with altitude, while $b(r)$ is rather steady around 0.5. The solid lines (green and red) in Figure 3b are exponential least squares fits to the parameters $a(r)$ and $b(r)$, respectively. The electron density seems to be sensitive to SZA all the way up to 2400 km, and the scale factor (the parameter $a(r)$) smoothly decreases with altitude. Above 2400 km the number of data points decrease and the measurement errors grow larger. It is not unexpected that the SZA dependence is strong at lower altitudes in a similar way as the solar EUV flux dependence, since both of these factors indicate how much sunlight is available to ionize the atmospheric neutrals.

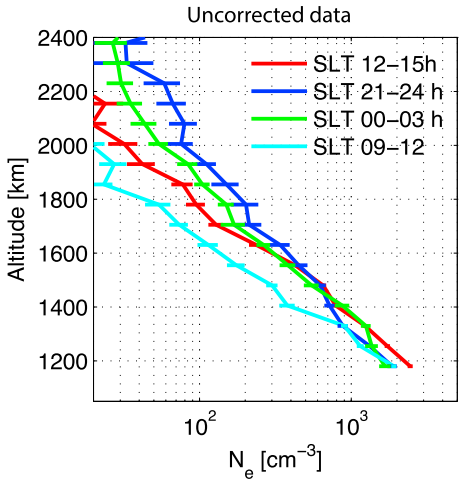

Figure 5. Same as Figure 4b except that the uncorrected data are used here.

As a second step we remove the SZA dependence by accounting for the SZA dependence at the altitude at which the measurements are made, according to

$$N_{e,\mathrm{SZA}}(r) = \frac{N_e(r)}{\cos(b(r) \cdot \theta_{\mathrm{SZA}})}, \tag{2}$$

where r is the altitude. $N_{e,\mathrm{SZA}}$ is now the SZA independent density and is plotted in Figure 3c with the same color coding for different altitude ranges as in Figure 3a.

As a next step we wish to remove the dependence on solar flux. According to Chapman theory, the density at a given altitude should be proportional to the ionizing flux $N_e \propto F_e^k$, where the exponent $k = 0.5$. Although the strict square root dependence appears to be valid at the ionospheric peak of Titan [*Edberg et al.*, 2013a], it might not be valid at higher altitudes in the ionosphere where photo ionization might not be the main controlling process or, more specifically, where photochemistry is not dominating over plasma transport processes or impact ionization processes or the dominant loss-process could be either recombination or attachment or where the ionospheric scale height increases at a higher rate than the plasma is produced. To investigate the dependence on solar flux at different altitudes, we plot the electron density as a function of solar energy flux F_e in 75 km altitude intervals from 1100 km up to 2400 km, in Figure 3d, in the same way as we did above for the SZA. We fit a linear curve (in lin-log space) of the form

$$n = cF^k, \tag{3}$$

to the data in each altitude interval. In Figure 3e we plot the parameters $c(r)$ and $k(r)$ as a function of altitude together with exponential fits. The error bars show the goodness of the fits. The ionosphere seems sensitive to EUV variations throughout the ionosphere, but the dependence gets weaker with altitude. As a next step we remove the solar EUV dependence and account for the EUV variations in order to get a EUV independent electron density according to

$$N_{e,\mathrm{EUV}}(r) = \frac{N_{e,\mathrm{SZA}}(r)}{c(r)F_e^{k(r)}} N_{\mathrm{max}}(r) \tag{4}$$

where $N_{\mathrm{max}}(r)$ is equal to the maximum density in each altitude interval. We multiply by this constant to get the density values to represent those of solar maximum conditions. $N_{e,\mathrm{EUV}} = N_{e,\mathrm{corrected}}$ is now the SZA and solar flux independent electron density.

As a third and final step we wish to remove the ram zenith angle dependence. We have performed in principle the same investigation as for the SZA and solar flux but found no clear trend of the electron density variation with the ram angle. Hence, we conclude that the ionospheric density is not particularly dependent on the ram angle in the altitude range up to 2400 km. Although a dependence could be seen for higher altitudes in Figure 2e, this dependence seems to have been removed when accounting for the solar energy flux and SZA variations.

The uncorrected electron density N_e is plotted as function of altitude in Figure 3g, and the final, corrected, electron density $N_{e,\mathrm{corrected}}$, which is in principle EUV and SZA (and ram angle) independent, is plotted in Figure 3h. This includes data from all flybys. As can be seen when comparing Figures 3g and 3f, some reduction in the variability of the data has occurred at the lower altitudes. At higher altitudes the density still shows rather great variability. The density has in general been shifted to higher values since in the two detrending steps described above, we have in principle shifted all the data to be that of maximum solar flux values and at the sub solar point (SZA = 0°).

Although the procedure to correct the data for biased sampling at different SZA and solar fluxes as described above is rather straight forward, it might not be the only way of correcting the data. A multiparameter fit would also have been an option but the approach described here should be sufficient for our purposes.

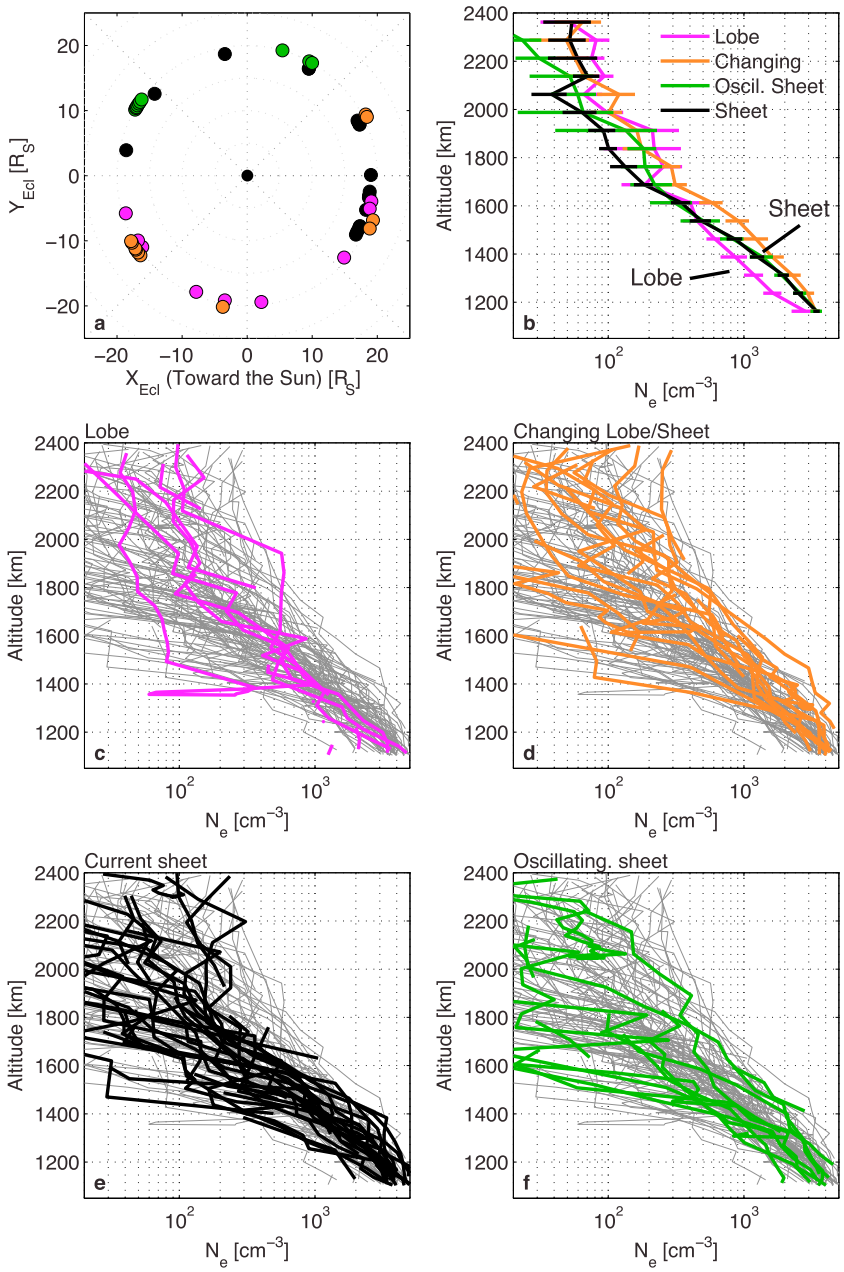

Figure 6. (a) Location of the Cassini Titan flybys shown projected on the *x-y* plane in the Saturn-centered ecliptic coordinate system. Note that the radial distances are shifted slightly to avoid plotting on top of each other. Now the colors correspond to in which Saturn magnetospheric ambient conditions the individual flyby occur in. (b) Altitude profiles of the mean electron density (in altitude intervals of 75 km) from all the data retrieved in the respective group of ambient conditions. The data is corrected for solar cycle and SZA variations. Note that if following the categorization by *Rymer et al.* [2009] and *Smith and Rymer* [2014], the sheet flybys have the overall highest mean density below 1600 km, rather than the "changing" category as shown here. (c—f) Each individual electron density altitude profile obtained by RPWS/LP from the group of ambient conditions. The grey lines show all obtained altitude profiles from the Cassini mission for easier comparison between panels.

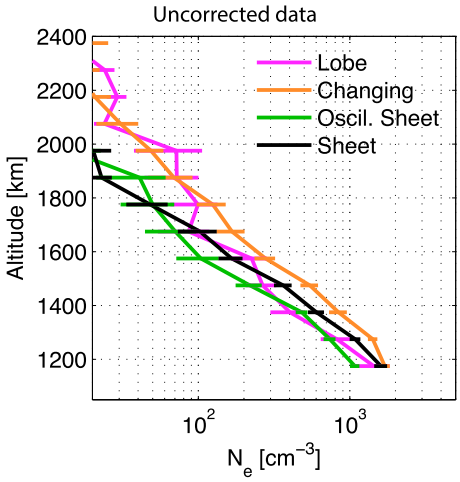

Figure 7. Same as Figure 6b except that the uncorrected data are used here.

We have tested the robustness of the above technique by altering the order of which parameter to correct for. Above we began by correcting for solar EUV flux followed by the SZA correction. If this order is changed, we end up with in principle the same end result, which gives some reassurance that what has been produced is correct. Also, if we change the bin sizes, the results do not deviate significantly.

4. Dependence on Saturn Local Time and Magnetospheric Conditions

Now that we have the electron density estimates independent of SZA and solar energy flux, we can start to investigate other possible sources, i.e., Saturn's magnetospheric variability, which could control the structure of Titan's ionosphere. We will investigate this by first studying how the Titan ionospheric density varies with SLT, since the ambient conditions are expected to, generally, be different at different sectors in Saturn's magnetosphere.

As the majority of all Titan flybys have occurred in four 3 h wide SLT sectors we naturally divide the individual Titan altitude profiles into four subsets, defined by those SLT sectors. The sectors are 00–03 h, 09–12 h, 12–15 h, and 21-00 h SLT and are illustrated in Figure 4a.

The flybys during which RPWS/LP gathered data in the SZA range 0°–120°, ram angle range 0°–120°, and altitude range 1100–2400 km and that occurred in the SLT = 00–03 h sector are T11 and T17–T23; in the SLT = 09–12 h sector: TA, TB, T3, T8, T36, T38–T45, and T47–T51; in the SLT = 12–15 h sector: T25–T31, T77, T83–84, and T86–96; and in the SLT = 21–00 h sector: T55–T59, T61, T62, T100, T104–105, and T107-109. In the postmidnight sector there were eight flybys from which we could use data and those occurred over a 6 month period from July 2006 to January 2007. In the prenoon sector there were 19 flybys ranging from October 2004 to March 2009. In the postnoon sector there were 25 flybys ranging from February 2007 to March 2014. And finally, in the premidnight sector there were 14 flybys, which occurred over two periods from May 2009 to October 2009 and from April 2014 to February 2015. We omit the T32, T85, and T96 flybys from this analysis since they are known to have occurred in the magnetosheath or in the solar wind.

In Figures 4c–4f we show the altitude profiles of the electron density from all flybys in each SLT sector, and in Figure 4b we show the mean density from all flybys in each SLT sector, calculated in 75 km altitude intervals. The error bars show standard error on the mean values. The premidnight and postmidnight flybys (blue and green lines) stand out in terms of having the highest electron density at altitudes above 1600 km compared to the profiles from other sectors. The mean values at the lowest altitudes (<1600 km) in Figure 4b are quite comparable between all four SLT sectors, although the postmidnight flybys (green line Figure 4b) show higher densities than in all other SLT sectors. The density measured when Titan is on the nightside of Saturn is higher than when Titan is on the dayside, even when including the error bars. This is valid at least above 1600 km. Note that Titan is still in sunlight, and photoionization is occurring, when located on Saturn's nightside.

In Figure 5 we show, for the sake of completeness, the same type of plot as in Figure 4b except for that we now display the uncorrected data (which is not detrended from SZA or solar energy flux and where the ionospheric peak has not been shifted). The Saturn nightside flybys show higher densities in this data set too, compared to the data from the flybys in the two dayside sectors.

Rather than separating each flyby by which SLT sector it occurs in, we have also sorted the flybys depending on the ambient conditions at the time of the flyby, as determined from the classifications provided by *Simon et al.* [2010] and *Simon et al.* [2013]. Those studies classified each flyby according to if it took place when Titan was in the magnetodisc current sheet, in the lobe of the magnetosphere (northern and southern), in an oscillating current sheet, or during a combination of several regimes. Some flybys were also unclassified due to unusual plasma or magnetic field signatures. (see Table 4 in *Simon et al.*, 2013). Presently, that table only includes flybys up to T85. We show the results in Figure 6, in the same format as Figure 4. There appears to be little effect on the Titan electron density structure above ~1600 km from the classifications of ambient conditions. However,

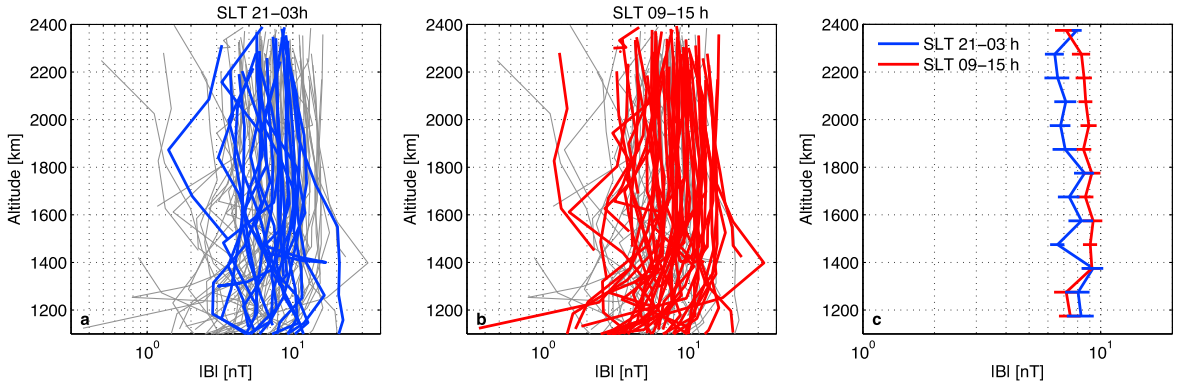

Figure 8. Altitude profiles of the magnetic field strength for the flybys occurring on (a) the nightside and (b) the dayside of Saturn as well as (c) the mean values of the field strength as a function of altitude of the two subsets. The grey lines in Figures 8a and 8b are altitude profiles from all flybys, for easy comparison between Figures 8a and 8b.

the densities are higher in the altitude interval 1100–1600 km when Titan is located in the sheet, compared to when in the lobe. This is in agreement with *Westlake et al.* [2011] who saw higher neutral densities in the sheet compared to when in the lobe. However, this result was debated by *Snowden et al.* [2013] who stated that no clear relation could be found between the neutral and the ionospheric conditions.

At higher altitudes there is no significant difference between the different ambient conditions, if taking into account the error bars, which again show standard error on the mean values. At the lower altitudes (below 1600 km), the flybys that are occurring under ambient conditions classified as changing, i.e., changing from the lobe to the sheet or vice versa, during a flyby, have the highest densities out of all categories. We note that most (but not all) of those flybys also occur on the Saturn nightside postmidnight.

In Figure 7 we show, again for the sake of completeness, the same type of plot as in Figure 6b except that we now display the uncorrected data (which is not detrended from SZA or solar energy flux and where the ionospheric peak has not been shifted). The Saturn lobe flybys do also show higher densities in this data set at low altitude, compared to the data from the flybys in the sheet sectors.

For the high altitudes, i.e., above about 1600 km, it appears as if the main dividing factor between low and high electron densities in Titan's ionosphere is whether Titan is located on the nightside or on the dayside of Saturn. (This is after having detrended from SZA and solar cycle effects). To investigate this further, we show in Figure 8 altitude profiles of the magnetic field strength $|B|$ as measured by MAG during each Titan flyby, including only data from ram angles less than 120°. We divide the data into nightside flybys (Figure 8a) and dayside flybys (Figure 8b), and in Figure 8c we show the mean values of the two subsets. Clearly, the magnetic field strength at altitudes above about 1600 km is higher when Titan is on the dayside of Saturn compared to when on the nightside, by about 2 nT or 25%. Hence, when we observe the electron density to be higher

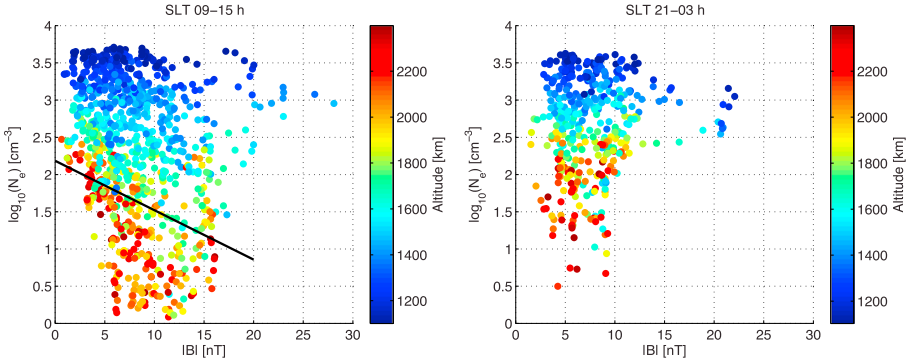

Figure 9. Magnetic field strength plotted as function of electron density and color coded by altitude. The data are divided into flybys occurring on the (left) dayside or (right) nightside of Saturn. The black line is a least squares fit to the data points in the altitude range 1600–2400 km. There is a trend of lower electron density for higher magnetic field in this altitude range.

than average, the magnetic field strength is observed to be lower and vice versa. In Figure 9 we show the electron density as a function of magnetic field strength and separated by nightside and dayside of Saturn. There is a visible trend of lower magnetic field strength with higher electron density, when the altitude is above 1600 km, for the Saturn dayside flybys but not for the nightside flybys.

5. Discussion

We have presented evidence of that the Titan ionospheric structure, above about 1600 km, is dependent on at what SLT Titan is located and, for Titan altitudes below 1600 km, in what the magnetospheric ambient conditions are. On the nightside of Saturn (SLT 21-03 h) the electron densities are a factor of ~2.5 higher than when on the dayside (SLT 09–15 h) for altitudes above 1600 km. When Titan is located in the sheet, the densities at altitudes below about 1600 km are a factor of 1.4 higher than when in the lobe, which is in agreement with results from *Westlake et al.* [2011].

For the higher altitudes, 1600–2400 km, the magnetic field strength also indicates a SLT dependence and is higher on the dayside of Saturn, where the electron density is lower than on the nightside. Conversely, the magnetic field strength around Titan is lower when on the nightside of Saturn where the electron density is higher. We interpret this as a consequence of the pressure balance between the magnetic pressure, $P_B = B^2/2\mu_0$, and the thermal pressure from the cold ionospheric plasma, $P_{th} = nk_BT$, which together should balance the sum of the dynamic pressure arising from the flow in Saturn's magnetosphere and the pressure from the energetic plasma in Saturn's magnetosphere. If the magnetic pressure increases, then the thermal pressure will decrease at that altitude in reaction to the total pressure. The thermal pressure above 1600 km is on average about a factor of 10 lower than the magnetic pressure [*Edberg et al.*, 2010]. If the magnetic pressure changes by 25%, then the thermal pressure will be affected, which is a likely scenario on the Saturn dayside where the solar wind pressure can cause the magnetic flux tubes to be compressed and the field strength to increase. On the Saturn nightside, there appears to be less of a correlation between the magnetic field pressure and the thermal pressure in the altitude range 1600–2400 km. Since the sum of the thermal and magnetic pressure is normally slightly lower than the dynamic pressure from the surrounding flow, there is less of pressure balance present on the nightside. The Saturn magnetospheric energetic plasma pressure can at times be the dominant pressure term at the orbit of Titan [*Sergis et al.*, 2009]. It has also been shown by *DeJong et al.* [2011] that there is a day/night asymmetry in the energetic electron fluxes, with higher fluxes on the nightside, which could lead to enhanced impact ionoization compared to when Titan is on the dayside. However, the day/night asymmetry reported by *DeJong et al.* [2011] was present at distances around 8 R_S from Saturn and so might not be relevant at the orbit of Titan.

For the lower altitudes in Titan's ionosphere, below 1600 km it has been determined that in order to cause additional ionization down to altitudes of 1100 km by electron impact ionization the energy required is less than 1 keV [*Cravens et al.*, 2005, 2006]. The increased density below 1600 km in Titan's ionosphere can therefore be explained by whether or not Titan is in the sheet where ~200 eV electrons are present. Generally, the highest density flybys occur when Titan is in the sheet or when there are rapid transitions between the sheet and the lobe, as can be seen in Figure 6b. The flybys that occur when Titan is in the lobe, where much fewer energetic electrons are present, show the overall lowest electron densities in the lower part of the ionosphere.

Furthermore, an additional source of particles capable of causing particle impact ionization could potentially come from reconnection events in the tail of Saturn. Titan is likely to be planetward of the average reconnection X line, and thus an additional source of energized ion flows (associated with dipolarization of the field that are traveling planetward from this downtail reconnection site) could be impacting on Titan. We do find most of the high-density altitude profiles in the same postmidnight sector as most of the signatures of reconnection, as observed from a vantage point tailward of the X line, have been found [*Jackman et al.*, 2014], which supports that explanation. However, the density in the premidnight sector is equally high, and few signatures of reconnection have been observed there. The lack of observations is partly because there have been fewer orbits in the deeper dusk regions.

Interestingly, four of the nine flybys in the postmidnight sector were "unclassified" in terms of what type of ambient magnetic field conditions was present and the magnetic environment during most of the flybys was dominated by what looked like frequent current sheet encounters and transitions from the northern to the southern lobe [*Simon et al.*, 2010]. There were, however, current sheet flappings and frequent transitions between lobe and current sheet during flybys in other SLT sectors too, but only one other flyby took place

during "unclassified" ambient conditions. From that it seems as if the ambient magnetic field in the postmidnight sector is quite variable, potentially indicating that there might be more tail dynamics, such as the current sheet flapping modeled by [*Arridge et al.*, 2011], in that sector than elsewhere.

Heating of the ionospheric plasma could possibly also cause the observed difference in the altitude profiles. Heating could occur during plasma injection events, which have been frequently observed at Saturn in terms of ENA emissions. Most of those events seem to peak premidnight and closer to about 10 R_S [*Carbary et al.*, 2008]. Still, the signatures seen premidnight could possibly indicate the presence of additional energization elsewhere in the magnetosphere and that would lead to ENA emissions in the premidnight sector and additional ionization or heating of Titan's upper atmosphere when on the nightside and further out, at 20 R_S. This is, however, rather speculative and cannot be confirmed by our measurements.

We do wish to point out that there are some uncertainties in the steps leading up to these results. The normalization of the data with respect to SZA and solar flux introduces further uncertainties, mainly arising from the assumption of constancy in the solar EUV output over the azimuthal rotation of the source region from sub-Earth to sub-Saturn. However, no alternative procedure exists for this calculation, and the effects of such short-term variations within the long-term study presented here are believed to be small, compared to the intrinsic variability of the ionosphere, and instrumental uncertainties associated with the Langmuir probe measurements. However, this uncertainty introduces an error that is smaller than the error bars from the mean values of the electron density altitude profiles. There is quite a large spread in density from one flyby to the next which should be taken into account when considering the results in this paper. Furthermore, we have made no attempt in trying to distinguish different ionospheric structures in the northern hemisphere compared to the southern hemisphere. This could potentially be important due to seasonal effects but will be hard to distinguish from the other controlling factors in Titan's ionosphere.

We have also looked at the ambient Saturn magnetospheric electron density, as determined by the "electron density proxy" method of *Morooka et al.* [2009] for all Titan flybys up until Aug 2010 (which is the latest date for which we have proxy data available). From that we cannot see any increased electron densities surrounding the nightside flybys, as compared to the dayside flybys.

We have also classified the flybys according to the scheme of *Rymer et al.* [2009] and *Smith and Rymer* [2014] who used plasma measurements rather than magnetic field measurements to determine which magnetospheric region Titan and Cassini are located in. That causes some flybys to be categorized differently from what *Simon et al.* [2010] and *Simon et al.* [2013] determined. The end result does, however, not differ much, and the sheet flybys still show higher densities than the lobe flybys at altitude below 1600 km. Interestingly, using the classification of *Rymer et al.* [2009] and *Smith and Rymer* [2014], we find that the flybys that occur in the sheet have the overall highest density, at altitudes below 1600 km, as opposed to the changing category in the classification by *Simon et al.* [2010] and *Simon et al.* [2013].

It is also possible that the neutral atmosphere background is different during some of the flybys. If the neutral densities would have been higher, then so would the ionospheric densities. If we, for instance, look at all the flybys surrounding the 6 month interval during which we have postmidnight sector flybys, regardless of in what SLT sector they occur, there is no visible trend of them all showing higher electron densities.

Although the highest mean density altitude profiles are found when Titan is on the nightside of Saturn, there is a considerable variability in the density profiles from flyby to flyby. Some flybys with high electron density profiles are, for instance, also found on the dayside. There are few low-density altitude profiles found on the nightside and especially not in the postmidnight sector, which suggests that additional ionization or heating is often more present there than in other SLT sectors.

6. Summary and Conclusions

We have shown that the ionospheric electron density of Titan, at altitudes above 1600 km, is generally higher when Titan is located on the nightside of Saturn, irrespective of what ambient magnetospheric conditions are present. For lower altitudes, below 1600 km, we find that the densities are higher when Titan is located in the magnetospheric current sheet of Saturn, compared to when in the lobe regions and irrespective of the SLT. These differences are present after we have corrected the data from biased sampling at different SZAs and solar energy flux. The difference in density between the nightside and the dayside is roughly a factor of 2.5. The difference between flybys in the sheet and in the lobe is approximately a factor of 1.4. We also find

that below 1600 km the highest densities, on average, occur when the ambient conditions are changing a lot, categorized as changing by *Simon et al.* [2010] and *Simon et al.* [2013]. This would suggest that additional fluxes of particles capable of impact ionization are impinging on Titan at these instances.

The observed difference in electron density at altitudes above 1600 km between flybys from the dayside and the nightside of Saturn is likely an effect of the combined thermal and magnetic pressure of the ionosphere balancing both the dynamic pressure of the corotating magnetospheric plasma and the energetic particle pressure. The magnetic pressure is higher on the dayside, due to the fact that the dynamic pressure with the solar wind compresses the magnetosheath and the magnetic flux tubes, which causes the thermal pressure (and the electron density) to decrease and to be relatively low on the dayside and high on the nightside. The observed difference in electron density between flybys in the magnetospheric sheet and in the lobe, at altitudes below 1600 km, is most likely caused by additional particle impact ionization from sheet electrons. When Titan is in the sheet region, the density in the deep ionosphere of Titan is generally higher compared to when Titan is in the lobe region.

Acknowledgments

D.J.A. and N.J.T.E. acknowledges funding from the Swedish Research Council and the Swedish National Space Board. The research at the University of Iowa was supported by NASA through contract 1415150 with the Jet Propulsion Laboratory. C.M.J.'s work at Southampton was supported by a Science and Technology Facilities Council Ernest Rutherford Fellowship. E.V. is grateful for funding from the Swedish National Space Board. The data available in this paper will be archived under the NASA/PDS archive and until then available upon request with the authors.

Larry Kepko thanks Philippe Garnier and one other reviewer for their assistance in evaluating this paper.

References

Achilleos, N., C. S. Arridge, C. Bertucci, C. M. Jackman, M. K. Dougherty, K. K. Khurana, and C. T. Russell (2008), Large-scale dynamics of Saturn's magnetopause: Observations by Cassini, *J. Geophys. Res.*, *113*, A11209, doi:10.1029/2008JA013265.

Ågren, K., et al. (2007), On magnetospheric electron impact ionisation and dynamics in Titan's ram-side and polar ionosphere—A Cassini case study, *Ann. Geophys.*, *25*, 2359–2369.

Ågren, K., J.-E. Wahlund, P. Garnier, R. Modolo, J. Cui, M. Galand, and I. Müller-Wodarg (2009), On the ionospheric structure of Titan, *Planet. Space. Sci.*, *57*, 1821–1827, doi:10.1016/j.pss.2009.04.012.

Ågren, K., N. Edberg, and J.-E. Wahlund (2012), Detection of negative ions in the deep ionosphere of Titan during the Cassini T70 flyby, *Geophys. Res. Lett.*, *39*, L10201, doi:10.1029/2012GL051714.

Arridge, C., et al. (2009), Plasma electrons in Saturn's magnetotail: Structure, distribution and energisation, *Planet. Space Sci.*, *57*(14–15), 2032–2047, doi:10.1016/j.pss.2009.09.007.

Arridge, C. S., N. Achilleos, and P. Guio (2011), Electric field variability and classifications of Titan's magnetoplasma environment, *Ann. Geophys.*, *29*(7), 1253–1258, doi:10.5194/angeo-29-1253-2011.

Backes, H., et al. (2005), Titan's magnetic field signature during the first Cassini encounter, *Science*, *308*, 992–995, doi:10.1126/science.1109763.

Bertucci, C., et al. (2008), The magnetic memory of Titan's ionized atmosphere, *Science*, *321*, 1475–1478, doi:10.1126/science.1159780.

Bertucci, C., D. C. Hamilton, W. S. Kurth, G. Hospodarsky, D. Mitchell, N. Sergis, N. J. T. Edberg, and M. K. Dougherty (2015), Titan's interaction with the supersonic solar wind, *Geophys. Res. Lett.*, *42*, 193–200, doi:10.1002/2014GL062106.

Bird, M. K., R. Dutta-Roy, S. W. Asmar, and T. A. Rebold (1997), Detection of Titan's ionosphere from Voyager 1 radio occultation observations, *Icarus*, *130*, 426–436, doi:10.1006/icar.1997.5831.

Carbary, J. F., D. G. Mitchell, P. Brandt, E. C. Roelof, and S. M. Krimigis (2008), Statistical morphology of ENA emissions at Saturn, *J. Geophys. Res.*, *113*, A05210, doi:10.1029/2007JA012873.

Coates, A. J. (2009), Interaction of Titan's ionosphere with Saturn's magnetosphere, *Philos. Trans. R. Soc. A*, *367*, 773–788, doi:10.1098/rsta.2008.0248.

Coates, A. J., F. J. Crary, D. T. Young, K. Szego, C. S. Arridge, Z. Bebesi, E. C. Sittler, R. E. Hartle, and T. W. Hill (2007), Ionospheric electrons in Titan's tail: Plasma structure during the Cassini T9 encounter, *Geophys. Res. Lett.*, *34*, L24S05, doi:10.1029/2007GL030919.

Cowley, S. W. H., E. J. Bunce, and R. Prangé (2004), Saturn's polar ionospheric flows and their relation to the main auroral oval, *Ann. Geophys.*, *22*(4), 1379–1394, doi:10.5194/angeo-22-1379-2004.

Crary, F. J., B. A. Magee, K. Mandt, J. H. Waite, J. Westlake, and D. T. Young (2009), Heavy ions, temperatures and winds in Titan's ionosphere: Combined Cassini CAPS and INMS observations, *Planet. Space. Sci.*, *57*, 1847–1856, doi:10.1016/j.pss.2009.09.006.

Cravens, T. E., et al. (2005), Titan's ionosphere: Model comparisons with Cassini Ta data, *Geophys. Res. Lett.*, *32*, L12108, doi:10.1029/2005GL023249.

Cravens, T. E., et al. (2006), Composition of Titan's ionosphere, *Geophys. Res. Lett.*, *33*, L7105, doi:10.1029/2005GL025575.

Cravens, T. E., I. P. Robertson, S. A. Ledvina, D. Mitchell, S. M. Krimigis, and J. H. Waite (2008), Energetic ion precipitation at Titan, *Geophys. Res. Lett.*, *35*, L03103, doi:10.1029/2007GL032451.

DeJong, A. D., J. L. Burch, J. Goldstein, A. J. Coates, and F. Crary (2011), Day-night asymmetries of low-energy electrons in Saturn's inner magnetosphere, *Geophys. Res. Lett.*, *38*, L08106, doi:10.1029/2011GL047308.

Dougherty, M. K., et al. (2004), The Cassini magnetic field investigation, *Space Sci. Rev.*, *114*, 331–383, doi:10.1007/s11214-004-1432-2.

Edberg, N. J. T., J.-E. Wahlund, K. Ågren, M. W. Morooka, R. Modolo, C. Bertucci, and M. K. Dougherty (2010), Electron density and temperature measurements in the cold plasma environment of Titan—Implications for atmospheric escape, *Geophys. Res. Lett.*, *37*, L20105, doi:10.1029/2010GL044544.

Edberg, N. J. T., K. Ågren, J.-E. Wahlund, M. W. Morooka, D. J. Andrews, S. W. H. Cowley, A. Wellbrock, A. J. Coates, C. Bertucci, and M. K. Dougherty (2011), Structured ionospheric outflow during the Cassini T55–T59 Titan flybys, *Planet. Space Sci.*, *59*, 788–797, doi:10.1016/j.pss.2011.03.007.

Edberg, N. J. T., D. J. Andrews, O. Shebanits, K. Ågren, J.-E. Wahlund, H. J. Opgenoorth, T. E. Cravens, and Z. Girazian (2013a), Solar cycle modulation of Titan's ionosphere, *J. Geophys. Res. Space Physics*, *118*, 5255–5264, doi:10.1002/jgra.50463.

Edberg, N. J. T., et al. (2013b), Extreme densities in Titan's ionosphere during the T85 magnetosheath encounter, *Geophys. Res. Lett.*, *40*, 2879–2883, doi:10.1002/grl.50579.

Fahleson, U., C. Fälthammar, and A. Pedersen (1974), Ionospheric temperature and density measurements by means of spherical double probes, *Planet. Space. Sci.*, *22*, 41–66, doi:10.1016/0032-0633(74)90122-6.

Garnier, P., et al. (2009), Titan's ionosphere in the magnetosheath: Cassini RPWS results during the T32 flyby, *Ann. Geophys.*, *27*, 4257–4272.

Garnier, P., M. K. G. Holmberg, J.-E. Wahlund, G. R. Lewis, S. R. Grimald, M. F. Thomsen, D. A. Gurnett, A. J. Coates, F. J. Crary, and I. Dandouras (2013), The influence of the secondary electrons induced by energetic electrons impacting the Cassini Langmuir probe at Saturn, *J. Geophys. Res. Space Physics*, *118*, 7054–7073, doi:10.1002/2013JA019114.

Gurnett, D. A., et al. (2004), The Cassini radio and plasma wave investigation, *Space Sci. Rev.*, *114*, 395–463, doi:10.1007/s11214-004-1434-0.

Jackman, C. M., J. A. Slavin, and S. W. H. Cowley (2011), Cassini observations of plasmoid structure and dynamics: Implications for the role of magnetic reconnection in magnetospheric circulation at Saturn, *J. Geophys. Res.*, *116*, A10212, doi:10.1029/2011JA016682.

Jackman, C. M., et al. (2014), Saturn's dynamic magnetotail: A comprehensive magnetic field and plasma survey of plasmoids and traveling compression regions and their role in global magnetospheric dynamics, *J. Geophys. Res. Space Physics*, *119*, 5465–5494, doi:10.1002/2013JA019388.

Lavvas, P., et al. (2013), Aerosol growth in Titan's ionosphere, *Proc. Natl. Acad. Sci.*, *110*(8), 2729–2734, doi:10.1073/pnas.1217059110.

Luhmann, J., et al. (2012), Investigating magnetospheric interaction effects on Titan's ionosphere with the Cassini orbiter ion neutral mass spectrometer, Langmuir probe and magnetometer observations during targeted flybys, *Icarus*, *219*(2), 534–555, doi:10.1016/j.icarus.2012.03.015.

McAndrews, H., et al. (2009), Plasma in Saturn's nightside magnetosphere and the implications for global circulation, *Planet. Space Sci.*, *57*(14–15), 1714–1722, doi:10.1016/j.pss.2009.03.003.

McAndrews, H., et al. (2014), Corrigendum to "Plasma in Saturn's nightside magnetosphere and the implications for global circulation" [Planet. Space Sci. 57 (14–15) (2009) 1714–1722], *Planet. and Space Sci.*, *97*, 86–87, doi:10.1016/j.pss.2014.05.011.

Medicus, G. (1962), Spherical Langmuir probe in drifting and accelerated Maxwellian distribution, *J. Appl. Phys.*, *33*, 3094–3100, doi:10.1063/1.1728574.

Mitchell, D. G., et al. (2005), Energetic ion acceleration in Saturn's magnetotail: Substorms at Saturn?, *Geophys. Res. Lett.*, *32*, L20S01, doi:10.1029/2005GL022647.

Morooka, M. W., et al. (2009), The electron density of Saturn's magnetosphere, *Ann. Geophys.*, *27*, 2971–2991.

Morooka, M. W., J.-E. Wahlund, A. I. Eriksson, W. M. Farrell, D. A. Gurnett, W. S. Kurth, A. M. Persoon, M. Shafiq, M. André, and M. K. G. Holmberg (2011), Dusty plasma in the vicinity of Enceladus, *J. Geophys. Res.*, *116*, A12221, doi:10.1029/2011JA017038.

Mott-Smith, H. M., and I. Langmuir (1926), The theory of collectors in gaseous discharges, *Phys. Rev.*, *28*, 727–763, doi:10.1103/PhysRev.28.727.

Rymer, A. M., H. T. Smith, A. Wellbrock, A. J. Coates, and D. T. Young (2009), Discrete classification and electron energy spectra of Titan's varied magnetospheric environment, *Geophys. Res. Lett.*, *36*, L15109, doi:10.1029/2009GL039427.

Sergis, N., S. M. Krimigis, D. G. Mitchell, D. C. Hamilton, N. Krupp, B. H. Mauk, E. C. Roelof, and M. K. Dougherty (2009), Energetic particle pressure in Saturn's magnetosphere measured with the magnetospheric imaging instrument on Cassini, *J. Geophys. Res.*, *114*, A02214, doi:10.1029/2008JA013774.

Shebanits, O., J.-E. Wahlund, K. Mandt, K. Ågren, N. J. Edberg, and J. Waite Jr. (2013), Negative ion densities in the ionosphere of Titan–Cassini RPWS/LP results, *Planet. Space Sci.*, *84*, 153–162.

Simon, S., A. Wennmacher, F. M. Neubauer, C. L. Bertucci, H. Kriegel, J. Saur, C. T. Russell, and M. K. Dougherty (2010), Titan's highly dynamic magnetic environment: A systematic survey of Cassini magnetometer observations from flybys TA–T62, *Planet. Space. Sci.*, *58*, 1230–1251, doi:10.1016/j.pss.2010.04.021.

Simon, S., S. C. van-Treeck, A. Wennmacher, J. Saur, F. M. Neubauer, C. L. Bertucci, and M. K. Dougherty (2013), Structure of Titan's induced magnetosphere under varying background magnetic field conditions: Survey of Cassini magnetometer data from flybys TA–T85, *J. Geophys. Res. Space Physics*, *118*, 1679–1699, doi:10.1002/jgra.50096.

Smith, H. T., and A. M. Rymer (2014), An empirical model for the plasma environment along Titan's orbit based on Cassini plasma observations, *J. Geophys. Res. Space Physics*, *119*, 5674–5684, doi:10.1002/2014JA019872.

Snowden, D., R. Yelle, J. Cui, J.-E. Wahlund, N. Edberg, and K. Ågren (2013), The thermal structure of Titan's upper atmosphere, I: Temperature profiles from Cassini INMS observations, *Icarus*, *226*(1), 552–582.

Thomsen, M. F., R. J. Wilson, R. L. Tokar, D. B. Reisenfeld, and C. M. Jackman (2013), Cassini/CAPS observations of duskside tail dynamics at Saturn, *J. Geophys. Res. Space Physics*, *118*, 5767–5781, doi:10.1002/jgra.50552.

Thomsen, M. F., C. M. Jackman, R. L. Tokar, and R. J. Wilson (2014), Plasma flows in Saturn's nightside magnetosphere, *J. Geophys. Res. Space Physics*, *119*, 4521–4535, doi:10.1002/2014JA019912.

Vigren, E., et al. (2013), On the thermal electron balance in Titan's sunlit upper atmosphere, *Icarus*, *223*, 234–251, doi:10.1016/j.icarus.2012.12.010.

Vigren, E., et al. (2015), Ionization balance in Titan's nightside ionosphere, *Icarus*, *248*, 539–546, doi:10.1016/j.icarus.2014.11.012.

Vuitton, V., R. V. Yelle, and M. J. McEwan (2007), Ion chemistry and N-containing molecules in Titan's upper atmosphere, *Icarus*, *191*, 722–742, doi:10.1016/j.icarus.2007.06.023.

Wahlund, J.-E., et al. (2005), Cassini measurements of cold plasma in the ionosphere of Titan, *Science*, *308*, 986–989, doi:10.1126/science.1109807.

Wahlund, J.-E., et al. (2009), On the amount of heavy molecular ions in Titan's ionosphere, *Planet. Space. Sci.*, *57*, 1857–1865, doi:10.1016/j.pss.2009.07.014.

Waite, J. H., D. T. Young, T. E. Cravens, A. J. Coates, F. J. Crary, B. Magee, and J. Westlake (2007), The process of tholin formation in Titan's upper atmosphere, *Science*, *316*, 870–875, doi:10.1126/science.1139727.

Wei, H. Y., C. T. Russell, M. K. Dougherty, Y. J. Ma, K. C. Hansen, H. J. McAndrews, A. Wellbrock, A. J. Coates, M. F. Thomsen, and D. T. Young (2011), Unusually strong magnetic fields in Titan's ionosphere: T42 case study, *Adv. Space Res.*, *48*, 314–322, doi:10.1016/j.asr.2011.02.009.

Wellbrock, A., A. J. Coates, G. H. Jones, G. R. Lewis, and J. Waite (2013), Cassini CAPS-ELS observations of negative ions in Titan's ionosphere: Trends of density with altitude, *Geophys. Res. Lett.*, *40*, 4481–4485, doi:10.1002/grl.50751.

Westlake, J. H., J. M. Bell, J. H. Waite Jr., R. E. Johnson, J. G. Luhmann, K. E. Mandt, B. A. Magee, and A. M. Rymer (2011), Titan's thermospheric response to various plasma environments, *J. Geophys. Res.*, *116*, A03318, doi:10.1029/2010JA016251.

Whipple, E. C., Jr. (1965), The equilibrium electric potential of a body in the upper atmosphere and in interplanetary space, PhD thesis, George Washington Univ., Washington, D. C.

Woods, T. N., F. G. Eparvier, S. M. Bailey, P. C. Chamberlin, J. Lean, G. J. Rottman, S. C. Solomon, W. K. Tobiska, and D. L. Woodraska (2005), Solar EUV Experiment (SEE): Mission overview and first results, *J. Geophys. Res.*, *110*, A01312, doi:10.1029/2004JA010765.